Quantification of Stromule Frequencies in Microscope Images of Plastids Combining Ridge Detection and Geometric Criteria

Birgit Möller[1] and Martin Schattat[2]

[1]*Pattern Recognition and Bioinformatics, Institute of Computer Science, Faculty of Natural Sciences III,*
Martin Luther University Halle-Wittenberg, Von-Seckendorff-Platz 1, 06120 Halle (Saale), Germany
[2]*Plant Organelle Shape and Dynamics Lab, Institute of Plant Physiology, Faculty of Natural Sciences I,*
Martin Luther University Halle-Wittenberg, Weinbergweg 10, 06120 Halle (Saale), Germany

Keywords: Plant Cells, Plastids, Stromules, Quantification, Segmentation, Ridge Detection, Geometric Criteria, ImageJ.

Abstract: Plastids are involved in many fundamental biochemical pathways in plants. They can produce tubular membrane out-folds from their surface. These so-called stromules have initially been described over a century ago, but their functional role is still elusive. To identify cellular processes or genetic elements underlying stromule formation screens of large populations of mutant plants or plants under different treatments are carried out and stromule frequencies are extracted. Due to a lack of automatic methods, however, this quantification is usually done manually rendering this step a main bottleneck in stromule research. Here, we present a new approach for quantification of stromule frequencies. Plastids are extracted from microscope images using local wavelet analysis over multiple scales combined with statistical hypothesis testing to resolve competing detections from different scales. Subsequently, for each plastid region evidence for the existence of stromules in its vicinity is investigated applying ridge detection techniques and geometric criteria. Experimental results prove that our approach is suitable to properly identify stromules. Even in microscopy images with a high noise level and distracting signals extracted stromule counts are comparable to those of biological experts.

1 INTRODUCTION

Fluorescent proteins have developed into an important cell biological tool. They have delivered evidence that membrane bound compartments in eukaryotic cells not only possess specific biochemical properties, but also specific shapes and numbers, and often exhibit striking dynamics. Life cell imaging revealed that these characteristics can drastically change in response to stress. Despite these clear and often strong responses it is still largely unknown how such changes support compartment function and how they are integrated into the cellular regulatory network.

Specifically interesting membrane bound compartments in this regard are plastids. Plastids are unique to plants and are involved in many fundamental biochemical pathways such as photosynthetic carbon fixation, which provides us with oxygen as well as food. Shapes of plastids vary between different plant tissues as well as plant species, but range usually from ellipsoid to almost perfectly spherical (Fig. 1A, B). In response to stimuli such as stress plastids can form surface membrane out-folds (Fig. 1C), so-called stromules (Köhler and Hanson, 2000). Although stromu-les are known to the scientific community for over a century and have been intensively studied by the use of fluorescent proteins for 20 years now, we still can only speculate about stromule function and regulation (Hanson and Hines, 2018).

An often used strategy to identify cellular processes or genetic elements important for stromules are screens in which larger populations (> 1000) of mutant plants are tested for altered stromule frequencies. The stromule frequency (or SF%) is defined as the percentage of plastids carrying at least one stromule (see also (Schattat and Klösgen, 2011)). In addition to genetic screens, screenings of different chemical inhibitors, hormones and peptides as well as of biotic or abiotic stresses for their ability to induce changes to the basic SF% are a common tool to study stromule regulation (see (Schattat and Klösgen, 2011; Gray et al., 2012) for examples). In order to reliably assess SF% of a single plant sample, such as a leaf, three to six randomly chosen spots of the sample are imaged, capturing up to 1500 plastids (precise number varies between plant species and tissues) of which the number of plastids with and without stromule has to be counted (e.g., (Schattat and Klösgen, 2011)).
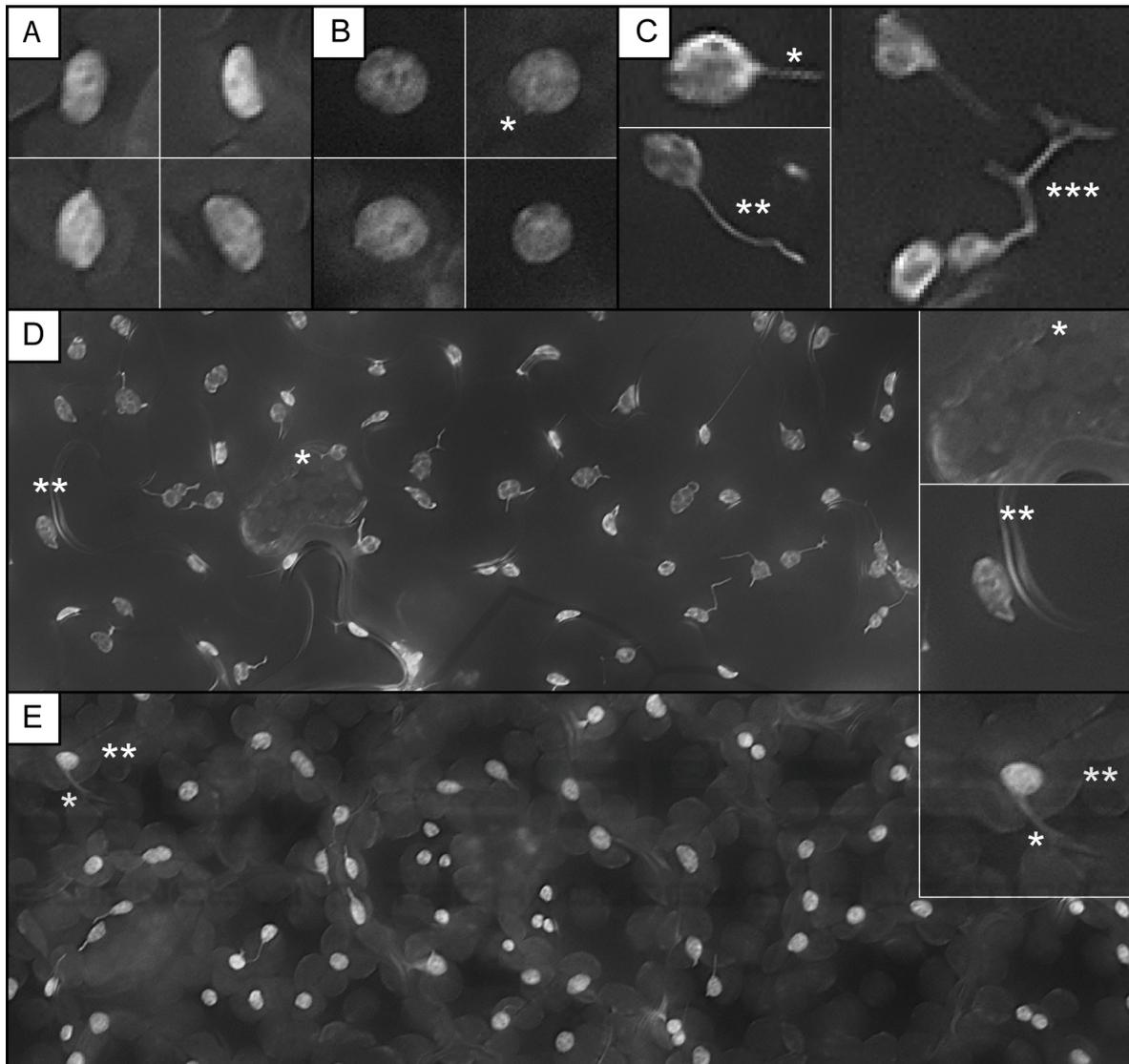
Figure 1: Sample image data: A, B) typical individual plastids lacking any stromules, A) four plastids exhibiting ellipsoid shapes (origin: upper leaf epidermis of *Arabidopsis thaliana*), B) four plastids being almost perfectly spherical (origin: lower leaf epidermis of *Nicotiana benthamiana*), B*) plastid exhibiting a very short spike-like stromule. C) Plastids exhibiting a straight (C*), curvilinear (C**) or branched (C***) stromule of intermediate length. D, E) representative sample images of flattened z-stacks of D) lower leaf epidermis (*N. benthamiana*) and E) upper leaf epidermis (*A. thaliana*). Insets (D*, D**, E* and E**) show details of inhomogeneous image background, spurious fluorescence signals, and reflections.

To record the shape of plastids, fluorescence proteins are targeted to the plastid stroma (Köhler et al., 1997; Marques et al., 2004) and imaged by fluorescence microscopy. Although automated microscope setups can easily generate large and representative image data sets, there is currently no computer-based tool available, which could assist with stromule quantification. Thus, the extraction of stromule frequencies still mainly relies on visual judgment (Schattat and Klösgen, 2011; Erickson et al., 2017; Kumar et al., 2018) and makes the assessment the current bottleneck in many stromule related projects. Therefore a tool for automated stromule frequency quantification would greatly support the advancement of stromule related research.

The automatic extraction of stromules from fluorescent microscopy images faces great challenges with regard to morphological properties and the overall appearance of stromules, their dynamic nature as well as concerning 3D image quality. Stromules exhibit a notable morphological diversity. In microscopy images stromules of medium and large size mostly

appear as long thin structures (Fig. 1C), while short stromules often subsume only a few pixels in length and appear as small spikes (Fig. 1B*). In addition, long stromules can be bent, kinked or even branched (Fig. 1C). Specifically under conditions inducing stromule formation, stromules can be highly dynamic and can change their shape as well as position in a matter of seconds. This can cause problems during z-stack recording, when stromules have time to move between consecutive frames, leading to imaging artefacts such as duplication of the respective stromule. However, recording of z-stacks spanning the entire cell is crucial for estimating SF% due to the central vacuole in plant cells and the rather dispersed nature of plastids and stromules. At the same time it is essential to image a larger number of cells in a sufficient quality and resolution, allowing not only to cover many plastids, but simultaneously allowing the detection of thin stromules reliably. Hence, the analysis of plastids and stromules demands for relatively fast 3D imaging data of high resolution.

Standard automated wide field fluorescence systems meet these necessities and are in some regards superior to confocal laser scanning setups, particularly concerning speed at higher image resolutions. However, wide field fluorescence images may contain distracting intensity signals from out of focus planes. This prevents the application of standard 3D image analysis strategies to such z-stacks and necessitates the projection into 2D images. For creating those projections no standard maximum projection method seems feasible, instead extending depth of field software such as CombineZP[1] (as described in (Schattat and Klösgen, 2009)) has to be used to create flattened 2D images (Fig. 1D, E). Despite harbouring the biological features of interest these extended wide field fluorescence images often suffer from imaging and projection artefacts such as inhomogeneous background and reflections on cell walls (Fig. 1D*, D**). Moreover, the artefacts often share significant similarities with stromules (Fig. 1D*, D**, E*, E**) and although they render the task of developing robust and automated image analysis tools challenging, the benefit of faster imaging speed at higher resolution makes wide field fluorescence images still the preferred choice for high-throughput work.

In this paper, we present a new image analysis workflow for quantifying stromule frequencies from wide field microscopy images facing these challenges. Plastids are robustly detected adopting the approach of (Greß et al., 2010) based on local wavelet analysis in a multi-scale framework. For localizing stromules in the vicinity of segmented plastids we apply ridge detection techniques to extract curvilinear segments as candidates for stromules. Subsequently, biological characteristics of stromules are exploited to define a set of geometric criteria suitable to distinguish between curvilinear segments referring to true stromules and segments originating from distracting image structures or reflections. Experimental results on images of different types of plastids prove that our new workflow is well-suited to ease the assessment of stromule frequencies even from challenging image data and marks an important progress towards fully automatic high-throughput analysis in this field.

The approach has been implemented in Java as part of MiToBo, a toolbox for processing and analyzing microscopy images (Möller et al., 2016), and the software is publically available. MiToBo seemlessly integrates into the widely used image analysis software ImageJ/Fiji (Schindelin et al., 2012; Rueden et al., 2017) and features its own ImageJ update site which grants direct access to all functionality and in particular to the new stromule analysis pipeline. MiToBo is open-source and released under GPL version 3.0, the source code of MiToBo and the new analysis pipeline, respectively, are available from MiToBo's website[2] and from Github.

The remainder of the paper is organized as follows. In Section 2 we review common techniques for the segmentation of cells and nuclei with similar characteristics like the plastids in our application, and for the extraction of curvilinear structures showing parallels to stromules. Our approach is outlined in Section 3 focusing on the new stromule detection method, before results and a conclusion are given in Section 4 and Section 5, respectively.

2 RELATED WORK

The task of segmenting plastid regions from 2D microscopy images is very specific, hence, established techniques for tackling this problem do not exist. Yet, the visual appearance of plastids in fluorescence microscopy images and their shape characteristics (Fig. 1) are comparable to those of small cells and nuclei. Accordingly, the problem of extracting plastid regions from 2D fluorescence microscope images is deeply linked to the segmentation of such objects (Chen et al., 2013; Buggenthin et al., 2013; Xing and Yang, 2016) as well as to the detection of particles and

---

[1]The CombineZP website is dead since August 2017, see https://en.wikipedia.org/wiki/CombineZ for details.

[2]MiToBo website, http://mitobo.informatik.uni-halle.de

larger spot-like structures on the cellular level (Basset et al., 2015). The variety of techniques applied for these problems is manifold, ranging from global or local image binarization in combination with morphological post-processing and often also a watershed transformation for separation of touching objects, to elaborate segmentation methods like graph cuts (Qi, 2014), levelsets (Bergeest and Rohr, 2012), and recently also techniques of deep learning (Kraus et al., 2016). The detection of spot-like structures (Smal et al., 2010) is often tackled with binarization and subsequent morphological post-processing, specific morphological operators like top hat, or h-dome transformations. Also frequency-based methods like wavelet analysis are common (Olivo-Marin, 2002).

Stromules are thin protrusions of varying length emenating from the surface of plastids. In the images of our application domain they appear as small curvilinear segments. The only published attempts to detect stromules from microscopy images have focused on detecting and tracking individual stromules in confocal microscope time series of individual plastids with the aim to identify stromule to microtubule interaction events (Kumar et al., 2018). Quantifications of stromule frequency in the same study were performed manually highlighting the absence of an available tool to quantify stromule frequency. In general stromules show a significant structural similarity to objects like vessels in retinal images (Fraz et al., 2012), streets in aerial imagery (Salahat et al., 2015), or roots in mini-rhizotron images (Zeng et al., 2008). For the segmentation of such structures various model-based approaches have been devised. Most of the time these aim at enhancing vessel-like structures based on model assumptions about their intensity profiles and structural appearance in images (Frangi et al., 1998; Staal et al., 2004; Moghimirad et al., 2012). The methods are often combined with subsequent segmentation techniques like thresholding. Some approaches (Steger, 1998) directly extract curvilinear structures by integrating initial localization of structures on the pixel level and subsequent linking procedures considering local neighborhoods.

3 METHODS

The aim of this work is to efficiently extract stromule frequencies SF% from microscopy images. To this end we seek to count the total number of plastids in an image from which at least one stromule emanates and which yields the basis for determining SF%. Hence, there is no need for accurately segmenting stromules in their full length. Rather, we focus on finding lo-

cal evidence of stromules in terms of thin curvilinear structures with coherent geometric properties in the vicinity of detected plastid regions.

Our workflow (Fig. 2) is separated in two phases and decouples plastid detection and identification of stromule parts. In the first phase (yellow box in Fig. 2) plastid regions are extracted from given input images adopting the method for robust detection of spot-like structures using wavelets from (Greß et al., 2010). In the second phase (green box in Fig. 2) each region is further examined to determine if there is evidence for the corresponding plastid to form a stromule or not.

3.1 Plastid Detection

Plastids appear in the flattened 2D images as circular to elliptical objects which on average show brighter intensities than the local background. For segmenting them from a given input image we adopt the approach of (Greß et al., 2010) aiming to extract spot-like and salient local regions from fluorescence microscopy images. The key idea of the method is to extract candidate regions by calculating and thresholding wavelet coefficients over multiple scales. Competing hypotheses for the same image location from different scales are resolved by statistical testing. Below we only briefly outline the basics of the method, for further details refer to (Greß et al., 2010).

Initially, the gray-scale input image is iteratively smoothed with steadily increasing mask sizes resulting in images of successively decreasing resolution. Wavelet coefficients are extracted as differences between pairs of smoothed images of adjacent scales. The coefficient images are thresholded applying a manually selected threshold, and foreground components are extracted from the binary images to identify locally striking intensity patterns as candidate regions for plastids. Since the thresholding is applied independently to each coefficient image, for a single image location competing plastid region hypotheses from different scales may result.

To select a single region as final segmentation result from each set of competing candidate regions statistical testing is used. It evaluates if a region is more likely related to a real plastid or originating from image noise. Given the null hypothesis that the local region originates from noise, this provides us with a statistical significance, i.e. a p-value, for each candidate region. The final detection result for each set of competing regions is then given by the candidate region associated with the smallest p-value, i.e. having the smallest probability to originate from image noise. Together with all regions distinctly detected at an image location this yields the final set of plastid
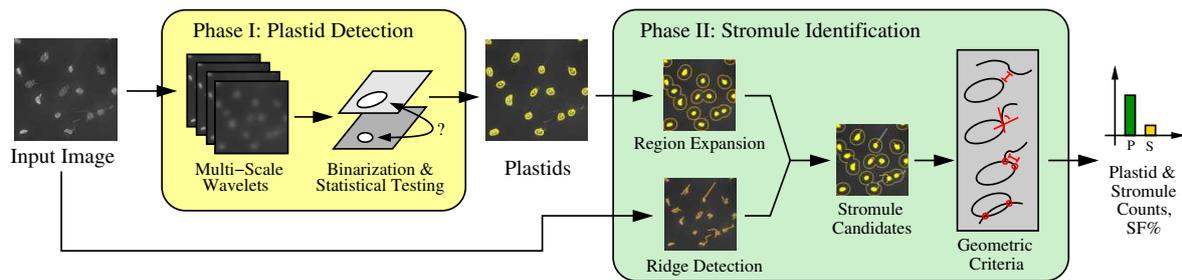
Figure 2: Overview of our approach: in the first phase (yellow box) plastid regions are extracted from input images, in the second phase (green box) curvilinear segments are detected in the vicinity of each plastid region and various geometric criteria are applied to classify them as referring to a stromule or originating from image artefacts and distracting signals.

regions forming the basis for the second step of stromule identification.

3.2 Stromuli Detection

If a stromule emenates from a plastid a thin and curvilinear structure is supposed to appear in the vicinity of the plastid region. We use a ridge detection method to localize candidates for such structures (Sec. 3.2.2). Due to the noise level in the flattened 2D images, inhomogeneous image background, spurious signals, and reflections, the ridge detection often yields a significant number of false-positive detections. Hence, we apply a collection of task-specific geometric criteria (Sec. 3.2.3) to exclude erroneously detected segments and decide about the presence of at least one stromule for each plastid region extracted in the first phase of our pipeline (Sec. 3.1). Since sometimes outstandingly bright stromule parts are falsely included in a plastid region during plastid detection, a pre-filtering step (Sec. 3.2.1) identifies such regions and applies complementary heuristics for stromule validation to these specific regions.

3.2.1 Pre-filtering of Plastid Regions

The plastid detection usually extracts the outlines of plastids accurately and yields compact and circular to elliptical regions. Very bright stromules, however, are sometimes detected as integral part of a plastid region. Then the basic assumptions about appearance and characteristics of stromules as outlined in the introduction and on which our detection methods relies are no longer valid. To handle such situations we perform a pre-filtering to identify detected regions not adhering to our model. Such regions are separately checked for the presence of stromules.

We first calculate the solidity of a plastid region as the ratio of its area and the area of its convex hull. If this ratio lies below 0.85 both areas significantly differ and further investigations are required. If parts of

a stromule have accidentally been included in a plastid region the shape of the region is locally thin and elongated. This property can be used as criterion for discovering such constellations. We extract the skeleton of a region under investigation, identify all end points and extract the corresponding branches from the end points up to the next branch or end point. All branches shorter than 5 pixels or with a distance of less than half of the total branch length between their end points are discarded. They are too short or form a circular structure very unlikely for stromules. Each of the remaining branches is searched for runs of consecutive pixels that have a distance smaller or equal to 4 pixels to the next background pixel in the binary region image. If the longest of these runs exceeds a length of 5 pixels the region is partially thin which is often a clear indication for the presence of a stromule.

3.2.2 Ridge Detection

For detecting curvilinear segments as candidates for stromule parts we use the ridge detection approach of Steger (Steger, 1998) with publically available source code[3]. Steger proposes models for the profiles of 1D and 2D curvilinear structures in images. Based on these models he derives criteria for the directional derivatives of the image function which need to be fulfilled by pixels along such structures and which serve as basis for segment extraction. Initially, respective pixels are found and for each pixel the local orientation of a potential segment is estimated from the eigenvalues and -vectors of the local Hessian matrix. Individual pixels are then linked to curvilinear segments considering the consistency of local orientation and user-defined contrast assumptions. The final result of the ridge detection is given by all curvilinear segments exceeding a minimal length threshold.

---

[3]Ridge (Line) Detection Plugin in Fiji by Wagner/Hiner, https://imagej.net/Ridge_Detection, accessed: 12/12/18
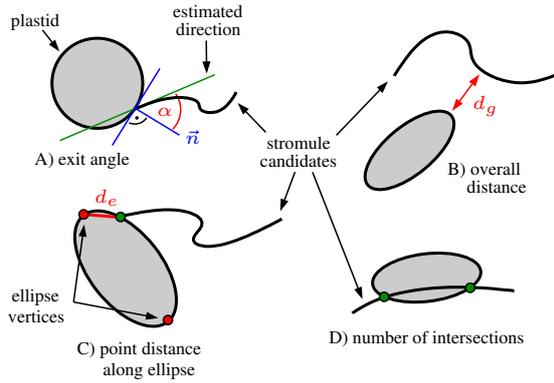
Figure 3: Geometric criteria to filter stromule candidates: they need to emanate from the surface almost perpendicular (A) and be located close to the plastid (B). In case of elliptical plastid regions they tend to start off close to the ellipse vertices (C) and usually do not cut through a region (D).

3.2.3 Geometric Criteria for Stromule Detection

The ridge detection usually yields a significant portion of false-positive stromule candidates, depending on noise level, image quality and potential artefacts due to the image acquisition process and the procedure for generating a flattened 2D image. Thus, to decide if a plastid region forms at least one stromule we need to further analyze the candidate segments.

According to the findings about the appearance of plastids and stromules in our application and as outlined in the introduction, we model each plastid region as an ellipse to enable the identification of stromules in their vicinity based on geometric criteria (Fig. 3). Besides general assumptions about the length of a stromule or its overall distance d_g to the plastid region (Fig. 3B), we mainly assume stromules to comply with two basic geometric criteria:

i) the angle α enclosed by the local normal $\vec{n}$ of the plastid surface and the direction of a potential stromule must not exceed a threshold θ_Δ (Fig. 3A), and

ii) for elliptical plastids the distance between the point of origin of a stromule and at least one vertex of the ellipse must not exceed a maximum distance θ_d (Fig. 3C).

In addition, stromules usually do not cut through a plastid region (Fig. 3D) which is a property well-suited to identify false detections due to reflections at the cell walls (cf. Fig. 1D**).

The different criteria outlined above are implemented in our workflow as follows. First, we select from the results of the ridge detection for each re-

gion the subset of segments which are located close enough to the region to be eligible as a potential stromule part. To this end, we define a focus area around each binary plastid region by iteratively expanding the region via morphological dilation to a maximal expansion of 20 pixels. In doing so region identity is preserved, i.e., dilation locally stops as soon as other regions are touched. Subsequently, all curvilinear segments are found which overlap with the expanded region. Segments can be assigned to multiple regions since a unique decision is not yet possible.

An ellipse is fit to each region to enable the application of the geometric criteria. Each point (x, y) on an ellipse in normal position, i.e., located in the center of the coordinate system with major and minor axes of lengths a and b, respectively, and being oriented parallel to the x- and y-axes of the coordinate system fulfills the following condition:

$$\varepsilon(x,y) := \left(\frac{x}{a}\right)^2 + \left(\frac{y}{b}\right)^2 = 0 \qquad (1)$$

For points located inside the ellipse $\varepsilon(x,y) < 0$ and for points located outside $\varepsilon(x,y) > 0$.

Given these definitions for each plastid region and each assigned segment we determine the number of intersections and classify the pixels of the segment according to their distance and relative location to the ellipse. Pixels of a segment located inside the ellipse or having a distance larger than 4 pixels to the ellipse are ignored in the following. Since the ellipses of the plastid regions are usually not in normal position pixels and ellipses are shifted and rotated to normal position prior to classifying the pixels. In addition, to account for discretization effects outer points are required to fulfill $\varepsilon(x,y) > 1$ instead of $\varepsilon(x,y) > 0$. If there are no such pixels found on a segment it is completely discarded. Also, if two or more intersections with the region ellipse are found the curvilinear segment is no longer considered since stromules usually do not cross through a plastid region.

For the remaining segments the checks for a small exit angle of the stromule and a short distance to the ellipse vertices are applied. To calculate the exit angle we determine the intersection point of ellipse and segment. In some cases no intersection point exists, e.g., due to discretization or if parts of a stromule could not be localized by the ridge detection due to a lack in contrast. Then we find the closest points on the ellipse and on the segment, respectively. Subsequently, we compute the local normal direction of the ellipse at the corresponding point and estimate the orientation of the segment by computing the orientation of a line through the neighboring pixels of the closest segment point (Fig. 3A). Since stromules usually emanate more or less perpendicular from the plastid sur-

face the angle α between both lines must not exceed a threshold θ_Δ. Finally, for elliptical plastids the minimal distance between the intersection point or the point with minimal distance to the ellipse, respectively, and any of the two vertices of the ellipse is calculated. If this distance lies below a threshold θ_d and there is still a segment part of at least three pixels length starting from the intersection point which lies outside of the ellipse a stromule is assumed.

In conclusion, each plastid region for which at least one of the candidate segments survives all the geometric checks is assumed to form a stromule. The stromule frequency (SF%) of an image is finally defined as the ratio of plastids which form at least one stromule in relation to all plastid regions detected in the image.

4 RESULTS

The plastid detection has already been publically released some time ago as integral part of the MTBCellCounter[4], a semi-automatic tool for counting cells and sub-cellular structures implemented as plugin in ImageJ/Fiji (Franke et al., 2015) and based on MiToBo (Möller et al., 2016). The stromule detection has been realized as extension for this tool, hence, is also publically available. The source code is released under GPL license and available from Github, additional documentation can also be found on the MiToBo website[5].

We have tested our approach on a set of images of the leaf epidermis from two different plants, *Arabidopsis thaliana* (Fig. 4) and *Nicotiana benthamiana* (Fig. 5). The MTBCellCounter was executed in an up-to-date Fiji installation on a virtual machine using a single core of an up-to-date desktop CPU and 2GB RAM, and running Windows 8, 64-bit, as operating system. Given these settings processing a single image takes on average a few seconds to approximately half a minute of time, depending on the chosen parameter settings (see below), the number of plastids present in the image, and of course the overall image quality and noise level. In general, the code is not yet optimized for efficiency and some intermediate steps might be speeded-up. Also, as each individual plastid region is processed independent of other regions parallelization of stromule analysis would be possible.

The MTBCellCounter allows to adjust the parameter settings for the plastid detection depending on

the concrete images at hand. In addition, the three geometric criteria applied in stromule validation which consider the number of intersections, the angle between surface normal and segment, and the distance to the ellipse vertices, can independently be enabled or disabled according to the type of plastids present in a specific experiment. Also the thresholds for the maximal difference in orientation and the vertex distance can individually be configured by the user.

We selected the images of our test set for which we present results here to show a significant variability in image characteristics allowing to demonstrate the general capabilities and flexibility of our approach. As a consequence the optimal settings for the various parameters were selected individually for each image. In common image data sets, however, the variance among individual images is usually much smaller than in the test data set and the images show more similar properties. Hence, in a more realistic experimental setting a common set of parameters for all images of a data set can be found easier and with moderate effort.

In Fig. 4 results for a section of one of the images of the upper epidermis of *Arabidopsis thaliana* are shown. In the top row the basis data for stromule identification, i.e., detected plastids (Fig. 4B) and extracted stromule candidate segments (Fig. 4D) are depicted. In this example all plastids have satisfactorily been detected. From the initial result of the ridge detection in Fig. 4C the high false-positive rate is obvious. Particularly in the image background several curvilinear structures have been found which are hard to distinguish from real stromules considering the local support of the ridge detection. After filtering out segments not located close to a plastid, however, many of the false-positives are already eliminated.

In the bottom row of Fig. 4 the outcomes of the different checks for geometric consistency are visualized. Plastid regions for which at least one stromule is hypothesized are shown in green color with the corresponding stromule parts being colored in yellow (irrelevant pixels inside the ellipse or too far away) and magenta (relevant pixels), respectively. Four of the seven plastids in this image form stromules, the three around the center of the image and the one in the bottom left corner. By applying just the exit angle criterion with $\theta_\Delta = 30°$ (Fig. 4E) three of these plastids are correctly identified, while in the top left corner an additional plastid is falsely assumed to form a stromule. If in addition also an ellipse distance threshold of $\theta_d = 3.0$ is applied (Fig. 4G) this false-positive detection is eliminated. The inset in Fig. 4G visualizes this criterion in detail for a different plastid. In orange and marked with white arrows you can see the ellipse
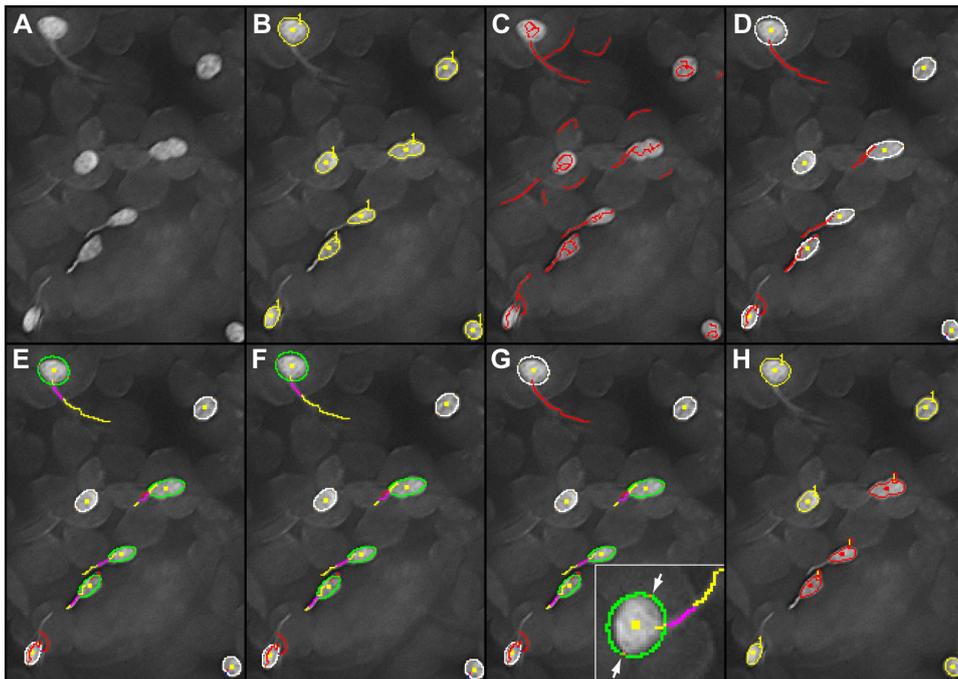
Figure 4: Results for images of *A. thaliana*: A) part of a typical input image; B) detected plastids; C) result of ridge detection; D) remaining stromule candidates; E) detected stromules with an exit angle less than 30°; F) result with multi-intersection check enabled in addition (here no effect); G) same result as in F) with additional ellipse distance threshold applied; H) final output with plastids (yellow) and plastids with stromules (red). For additional information on color encodings refer to the text.

vertices which in this case are relatively far away from the exit point of the potential stromule on the right. The stromule visible in the bottom left corner cannot be identified in this example due to a lack in contrast and some blurring around its exit point which already causes the ridge detection to fail here (Fig. 4C).

In Fig. 5 a sample detection result for an image clip from one of the images of *Nicotiana benthamiana* is shown. Compared to *Arabidopsis thaliana* the plastids in *Nicotiana benthamiana* are usually more circular, hence, the distance criterion assuming stromule exit points being located close to the ellipse vertices does not work well in this case. In addition, reflections at cell walls occur more frequently in these images. The plastid detection again detects all three plastids in this example (Fig. 5B) very accurately. Only the plastid in the bottom left corner forms a stromule while the one in the center of the image is located close to a reflection. From the results of the ridge detection it can be seen that for both, the reflection and the true stromule, candidate segments are detected. Without applying the check for multiple intersections both are classified as stromule parts (Fig. 5D), while enabling the criterion yields the correct result with only one plastid forming a stromule here (Fig. 5E, F). The criterion for the distance between ellipse vertices and exit point could also help

to eliminate the false-positive detection in this specific case. However, generally enabling the criterion for images of *Nicotiana benthamiana* bears the risk to exclude many true stromule candidates due to the shape characteristics of the plastids.

Our data set of test images subsumes in total 6 images of *Arabidopsis thaliana* and 6 images of *Nicotiana benthamiana*. For all 12 images an automatic detection of plastids and stromules was carried out applying our new workflow. Subsequently, the results were manually checked and partially corrected by a biological expert yielding an estimate for the accuracy of automatic quantification. In Fig. 6 scatter plots of automatic and manual counts for plastids (at the top) and stromules (at the bottom) are shown. As can be seen from the plots our approach tends to slightly larger counts for plastids and stromules than resulting from manual annotation, though, the absolute differences are usually smaller than 10. For stromules slightly larger differences can be observed. This is mainly due to stromules being much more difficult to detect than plastids. Particularly distracting intensity signals like reflections or others curvilinear structures also present in the images may easily result in false detections. Nonetheless extracted stromule frequencies usually coincide well between manual and automatic counting.
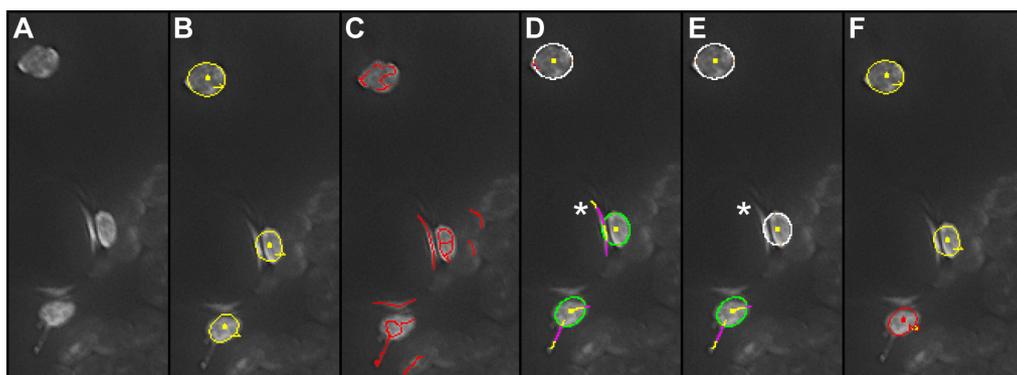
Figure 5: Results for images of *N. benthamiana*: A) part of a typical input image; B) detected plastid regions; C) result of the ridge detection; D) detected stromules with one reflection (D*) being erroneously classified as stromule; F) result with activated multi-intersection criterion which eliminates the false-positive detection (E*); F) final output with detected plastids (yellow) and plastids forming stromules (red).
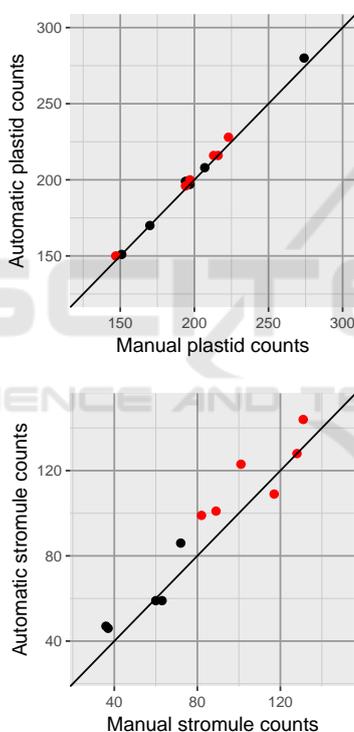
Figure 6: Result counts for the 12 test images (black: *A. thaliana*, red: *N. benthamiana*), on top plastids and at the bottom stromules. On the x-axes the counts manually extracted by a biological expert are shown, on the y-axes the counts automatically acquired with our new workflow.

In Fig. 7 extracted stromule frequencies for each of the 12 test images are plotted, the results of the automatic extraction in red and the ones of the manual extraction in black. The overall stromule frequencies (SF%) vary significantly between the different images where in this case images of *Nicotiana benthamiana* (bars on the right) show larger frequencies than the images of *Arabidopsis thaliana* (bars on the left) due to different treatments. The automatically and manually extracted stromule frequencies are most of the time comparable with an average difference of ≈ 0.062. For three images (IDs 2, 9 and 10) the differences exceed 0.1 with a maximum of ≈ 0.15. Vice versa, for five images the difference lies below 0.05.
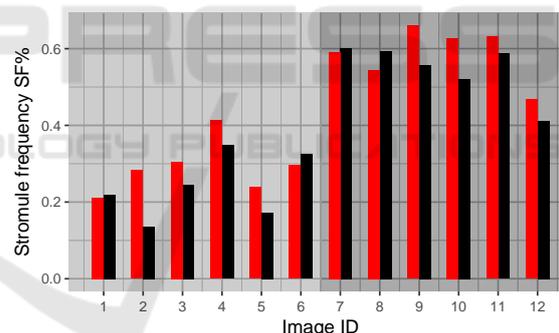
Figure 7: Comparison of automatically (red) and manually (black) extracted stromule frequencies for the 12 images of *A. thaliana* (IDs $1-6$) and *N. benthamiana* (IDs $7-12$).

Given the unquestionable difficulty of the overall task of stromule identification in wide field fluorescence microscopy images, and given the observation that also within the manual counting results of different human experts usually noticeable variation in the numbers of plastids and particularly of stromules can be observed, the results appear very pleasing. Certainly the quality of the detection depends on the overall image characteristics, and large variability within a set of images renders the task of stromule identification harder. Nevertheless, as could be shown by the experimental results in this study the approach can already satisfactorily cope with a significant amount of variation and will allow to extract reasonable stromule

frequencies in many settings. In addition, the overall time required for checking and post-processing the results of the new automatic workflow will in almost all cases be significantly smaller than the time necessary for fully manual annotation of plastids and stromules. Instead of manually annotating several hundreds of plastids and stromules by hand, usually only up to 15% of the plastids and an even smaller fraction of plastids with stromules per image requires manual processing. This allows to extract large and representative data sets much more efficiently than before yielding a suitable basis for biological investigations.

5 CONCLUSIONS

The new image analysis workflow for the extraction of stromule frequencies from wide field microscopy images is capable of extracting reasonable quantitative data suitable for biological investigations. Its performance is comparable to those of human experts while greatly reducing the time requirements. The necessity for manual intervention is significantly reduced to a small fraction of the time that would be necessary for fully manual annotation. Thus, although the overall workflow is not yet fully automatic and relies on manual parameter tuning as well as on manual validation and post-processing of results, our approach marks a significant improvement over the state-of-the-art in stromule studies.

Future work will aim to further increase the degree of automation and improve overall computational efficiency and detection robustness, particularly with regard to stromules. One possible direction will be the investigation of machine learning techniques for robust stromule identification particularly in images with a high noise level and low quality.

ACKNOWLEDGEMENTS

REFERENCES

Basset, A., Boulanger, J., et al. (2015). Adaptive spot detection with optimal scale selection in fluorescence microscopy images. *IEEE Trans. on Image Proc.*, 24(11):4512–4527.

Bergeest, J.-P. and Rohr, K. (2012). Efficient globally optimal segmentation of cells in fluorescence microscopy images using level sets and convex energy functionals. *Medical Image Analysis*, 16(7):1436 – 1444.

Buggenthin, F., Marr, C., et al. (2013). An automatic method for robust and fast cell detection in bright field images from high-throughput microscopy. *BMC Bioinformatics*, 14(1):297.

Chen, C., Wang, W., et al. (2013). A flexible and robust approach for segmenting cell nuclei from 2D microscopy images using supervised learning and template matching. *Cytometry Part A*, 83A(5):495–507.

Erickson, J. L., Adlung, N., et al. (2017). The Xanthomonas effector XopL uncovers the role of microtubules in stromule extension and dynamics in nicotiana benthamiana. *The Plant Journal*, 93(5):856–870.

Frangi, A. F., Niessen, W. J., et al. (1998). Multiscale vessel enhancement filtering. In *Medical Image Computing and Computer-Assisted Intervention (MICCAI)*, pages 130–137. Springer Berlin Heidelberg.

Franke, L., Storbeck, B., et al. (2015). The 'MTB Cell Counter' a versatile tool for the semi-automated quantification of sub-cellular phenotypes in fluorescence microscopy images. A case study on plastids, nuclei and peroxisomes. *Journal of Endocytobiosis and Cell Research*, 26:31–42.

Fraz, M., Remagnino, P., et al. (2012). Blood vessel segmentation methodologies in retinal images - a survey. *Computer Methods and Programs in Biomedicine*, 108(1):407–433.

Gray, J. C., Hansen, M. R., et al. (2012). Plastid stromules are induced by stress treatments acting through abscisic acid. *The Plant Journal*, 69(3):387–398.

Greß, O., Möller, B., et al. (2010). Scale-adaptive wavelet-based particle detection in microscopy images. In Meinzer, H.-P., Deserno, T. M., Handels, H., and Tolxdorff, T., editors, *Bildverarbeitung für die Medizin*, Informatik Aktuell, pages 266–270, Berlin. Springer. ISBN 978-3-642-11967-5.

Hanson, M. R. and Hines, K. M. (2018). Stromules: probing formation and function. *Plant Physiology*, 176(1):128–137.

Köhler, R. H., Cao, J., et al. (1997). Exchange of protein molecules through connections between higher plant plastids. *Science*, 276(5321):2039–2042.

Köhler, R. H. and Hanson, M. R. (2000). Plastid tubules of higher plants are tissue-specific and developmentally regulated. *Journal of Cell Science*, 113:81–89.

Kraus, O. Z., Ba, J. L., and Frey, B. J. (2016). Classifying and segmenting microscopy images with deep multiple instance learning. *Bioinformatics*, 32(12):i52–i59.

Kumar, A. S., Park, E., et al. (2018). Stromule extension along microtubules coordinated with actin-mediated anchoring guides perinuclear chloroplast movement during innate immunity. *eLife*, 7:e23625.

Marques, J. P., Schattat, M. H., et al. (2004). In vivo transport of folded EGFP by the DeltapH/TAT-dependent pathway in chloroplasts of Arabidopsis thaliana. *Journal of Experimental Botany*, 55(403):1697–1706.

Moghimirad, E., Rezatofighi, S. H., and Soltanian-Zadeh, H. (2012). Retinal vessel segmentation using a multi-

scale medialness function. *Computers in Biology and Medicine*, 42(1):50–60.

Möller, B., Glaß, M., et al. (2016). MiToBo - a toolbox for image processing and analysis. *Journal of Open Research Software*, 4(1):e17.

Olivo-Marin, J.-C. (2002). Extraction of spots in biological images using multiscale products. *Pattern Recognition*, 35(9):1989 – 1996.

Qi, J. (2014). Dense nuclei segmentation based on graph cut and convexity-concavity analysis. *Journal of Microscopy*, 253(1):42–53.

Rueden, C. T., Schindelin, J., et al. (2017). ImageJ2: ImageJ for the next generation of scientific image data. *BMC Bioinformatics*, 18(1):529.

Salahat, E., Saleh, H., et al. (2015). Novel MSER-guided street extraction from satellite images. In *IEEE Intern. Geoscience and Remote Sensing Symp. (IGARSS)*, pages 1032–1035.

Schattat, M. H. and Klösgen, R. B. (2009). Improvement of plant cell microscope images by use of "depth of field"-extending software. *Journal of Endocytobiosis and Cell Research*, (19):11–19.

Schattat, M. H. and Klösgen, R. B. (2011). Induction of stromule formation by extracellular sucrose and glucose in epidermal leaf tissue of arabidopsis thaliana. *BMC Plant Biology*, 11(1):115.

Schindelin, J., Arganda-Carreras, I., et al. (2012). Fiji: an open-source platform for biological-image analysis. *Nature Methods*, 9(7):676.

Smal, I., Loog, M., et al. (2010). Quantitative comparison of spot detection methods in fluorescence microscopy. *IEEE Trans. on Medical Imaging*, 29(2):282–301.

Staal, J., Abràmoff, M. D., et al. (2004). Ridge-based vessel segmentation in color images of the retina. *IEEE Transactions on Medical Imaging*, 23:501–509.

Steger, C. (1998). An unbiased detector of curvilinear structures. *IEEE Trans. Pattern Anal. Mach. Intell.*, 20(2):113–125.

Xing, F. and Yang, L. (2016). Robust nucleus/cell detection and segmentation in digital pathology and microscopy images: a comprehensive review. *IEEE Reviews in Biomedical Engineering*, 9:234–263.

Zeng, G., Birchfield, S. T., and Wells, C. E. (2008). Automatic discrimination of fine roots in minirhizotron images. *New Phytologist*, 177(2):549–557.